Original Research

CFTR deficiency aggravates Ang II induced vasoconstriction and hypertension by regulating Ca^{2+} influx and RhoA/Rock pathway in VSMCs

Liyan Zhao[1,2,†], Feng Yuan[2,†], Ni Pan[2], Yun Yu[3], Hanyan Yang[2], Yaosheng Liu[2], Ruomei Wang[4], Bin Zhang[5,*], Guanlei Wang[2,*]

[1]*Department of Pharmacy, the First Affiliated Hospital of Sun Yat-sen University, 510080 Guangzhou, Guangdong, China,* [2]*Department of Pharmacology, Zhongshan School of Medicine, Sun Yat-sen University, 510080 Guangzhou, Guangdong, China,* [3]*Department of Ophthalmology, Sun Yat-sen Memorial Hospital, Sun Yat-sen University, 510120 Guangzhou, Guangdong, China,* [4]*School of Data and Computer Science, Sun Yat-sen University, 51006 Guangzhou, Guangdong, China,* [5]*Guangdong Cardiovascular Institute, Guangdong Provincial People's Hospital, Guangdong Academy of Medical Sciences, 510080 Guangzhou, Guangdong, China*

TABLE OF CONTENTS

Submitted: 28 September 2021 Revised: 4 November 2021 Accepted: 9 November 2021 Published: 30 December 2021

1. Abstract

Background: Cystic fibrosis transmembrane conductance regulator (CFTR) has been associated with vascular tone and blood pressure (BP), however, its role in the genesis of hypertension remains elusive. In the present study, we investigated the regulating effect of CFTR on angiotensin II (Ang II) -induced hypertension and defined the molecular role of CFTR in vasoconstriction. **Results**: We found that CFTR mRNA and protein expression were markedly down-regulated in the arteries from Ang II induced hypertensive animals. During the development of hypertension, BP of *Cftr*$^{-/-}$ mice was significantly higher than that of *Cftr*$^{+/+}$ mice. Arteries from *Cftr*$^{-/-}$ mice or pre-incubated with CFTR specific inhibitor CFTR(inh)-172 exhibited a greater contractile response to Ang II. In vascular smooth muscle cells (VSMCs), the phosphorylation of myosin light chain (MLC), which is the core of VSMCs contraction, was negatively modulated by CFTR. Furthermore, intracellular Ca^{2+} concentration ($[Ca^{2+}]_i$) rise in response to Ang II was negatively modulated by CFTR, while no alteration was observed in resting VSMCs. Ras homolog family member A/Rho-associated protein kinase (RhoA/Rock) mediated phosphorylation of myosin phosphatase target subunit 1 (MYPT1), a regulator of MLC phosphorylation, was negatively modulated by CFTR in both resting and Ang II-stimulated VSMCs. **Conclusions**: This study demonstrates that CFTR is a negative regulator of vasoconstriction and hypertension, and the underlying mechanism contains two possible pathways: (1) in resting VSMCs, CFTR altered MLC phosphorylation through RhoA/Rock pathway; (2) in Ang II stimulated VSMCs, the regulating effect was mediated by both Ca^{2+} influx and RhoA/Rock mediated pathway.

2. Introduction

Hypertension is a critical risk factor for cardiovascular disease, which is the leading cause of death and disability worldwide. Angiotensin II (Ang II), as the major bioactive product of renin-angiotensin system, is crucial for salt and water homeostasis and vasoconstriction, and thus plays a critical role in the genesis of hypertension [1]. In vascular smooth muscle cells (VSMCs), activation of AT1 receptor by Ang II causes phospholipase C (PLC) activation, leading to the release of the second messengers inositol trisphosphate (IP_3) and diacylglycerol (DAG) and results in the rise of intracellular Ca^{2+} concentration ($[Ca^{2+}]_i$). Elevated $[Ca^{2+}]_i$ initiates a Ca^{2+}-calmodulin (CaM) interaction, causing the activation of myosin light chain kinase (MLCK) and the consequent phosphorylation of myosin light chain (MLC) [2]. MLC phosphorylation level is the core of VSMCs contraction, which depends on the balance between MLCK and MLC phosphatase (MLCP) activity. RhoA, a member of the Rho family of small GTPase binding proteins, is abundantly expressed in VSMCs. Activation of RhoA and its downstream target Rho-kinase (Rock) is increasingly being recognized as an important mechanism of vasoconstriction by Ang II. RhoA activation induces phosphorylation of myosin phosphatase target subunit 1 (MYPT1), which enhances the dephosphorylation of MLCP [2]. The reduction of MLCP activity increases the phosphorylation level of MLC, and thereby maintaining force generation in VSMCs. Deregulation of these cellular signaling components can lead to an overstimulated state causing sustained vasoconstriction and the elevation of blood pressure.

Several studies have identified Cl^- channels expression and characterized their function in vascular smooth muscle cells (VSMCs), including classic Ca^{2+}-activated Cl^- channel (CaCC), cGMP-dependent CaCC, volume regulated Cl^- channel (VRCC) and cystic fibrosis transmembrane conductance regulator (CFTR) [3]. Evidence from genetic and pharmacological studies point to a critical role for Cl^- channels during the development of hypertension [4]. Previous work in our laboratory have demonstrated that VRCC and CaCC were involved in VSMCs proliferation [5, 6] and cerebrovascular remodeling during hypertension [7–9]. CFTR is a member of the ATP-binding cassette transporter superfamily that functions as a Cl^- channel across the membrane. *Cftr* gene mutations lead to cystic fibrosis (CF) disease, which results in dysfunction of transepithelial movement of water and electrolyte in exocrine tissues [10]. Clinical data showed that older female CF mutation carriers exhibited lower blood pressure (BP), which had been attributed to excessive salt depletion [11]. Radiotelemetry measurements of physiological blood pressure demonstrated that average SBP and DBP of 24-hour of *Cftr*$^{-/-}$ mice were all significantly higher than those of *Cftr*$^{+/+}$ mice [12]. These previous studies indicated that CFTR might play an important role in BP control, however, the regulating effect of CFTR on the genesis of hypertension remains unclear.

Hypertension is pathologically characterized by augmented vascular contractility. The role of CFTR function has been described in smooth muscle cells of airway [13, 14], mesenteric artery [15] and aorta [16]. It was reported that trachea from CF patients showed greater MLC phosphorylation in response to IL-8 [17]. Previous studies on blood vessels showed that depolarization induced aortic tension was significantly increased in *Cftr*$^{-/-}$ mice compared to *Cftr*$^{+/+}$ mice [16]. CFTR corrector compounds (C18 or lumacaftor) normalize pathological alterations in cerebral arterial CFTR expression, vascular reactivity, and cerebral perfusion [18], suggesting that CFTR was involved in the regulation of vascular tone. Nevertheless, further research is needed to investigate the signaling mechanisms underlying the effect of CFTR on vasoconstriction during hypertension.

In the current study, Ang II infusion induced hypertensive models were established and the influence of *Cftr* knockout on BP during this process was investigated. CFTR protein mRNA/protein expression in the hypertensive arteries were examined. Besides, the regulating effect of CFTR on Ang II induced vasoconstriction was assessed *in vivo* with CFTR pharmacologically inhibited or genetically knockout. Furthermore, the underlying signaling mechanisms was investigated centered around the phosphorylation of MLC. This study reveals the specific involvement of CFTR in the regulation of vasoconstriction and genesis of hypertension.

3. Materials and methods

3.1 Animals

All animal care and experimental procedures complied with the policies of Ethics Committee of ZSSOM on Laboratory Animal Care (document No. 2016-080) and conformed to the "Guide for the Care and Use of Laboratory Animals" of the National Institute of Health in China. Sprague-Dawley rats were purchased from the Experimental Animal Center of Sun Yat-sen University. The gut-corrected *Cftr* knockout mouse strain STOCK $Cftr^{tm1Unc}$ Tg(FABPCFTR)1Jaw/J was purchased from the Jackson Laboratory (ME, USA). Females that are heterozygous for the *Cftr* knockout allele and homozygous for the FABP-hCFTR transgene were bred with males that are homozygous for both *Cftr* knockout allele and FABP-hCFTR transgene and thus wild-type ($Cftr^{+/+}$), heterozygote ($Cftr^{+/-}$) and Cftr knockout ($Cftr^{-/-}$) littermates were obtained. Animals were housed in standard plastic rodent cages and maintained at a regulated environment (25 °C, 12 h light, 12 h dark cycle with lights on at 7:00 and off at 19:00) with ad libitum access to a normal chow diet with 2.45 g NaCl/1000 g (D12450B, 10 kcal % Fat, Research Diets). The number used followed the principle of minimal requirement and showed in Figure legends.

Ang II induced hypertension models were established using $Cftr^{+/+}$, $Cftr^{-/-}$ mice (5–8 weeks old) or Sprague-Dawley rats (150–200 g). Ang II was administered via subcutaneously implanted osmotic minipumps (Alzet, Cupertino, CA, Model 1002 for mice and 2002 for rats) for 2 weeks to establish Ang II infusion induced hypertension models. The administration rate was 1000 ng/kg/min [19] for mice and 80 ng/min [20] for rats as previously reported and manufacture's instruction. BP was measured in conscious mice at 6:00 PM by tail cuff plethysmography (BP-98A, Softron, Japan) as we previously reported [21].

3.2 Reagents

Antibody to CFTR was from Alomone Labs (Jerusalem, Israel) and antibody to MLCK was from Sigma Aldrich Corp. (St. Louis, MO, USA). Antibodies to total myosin light chain (t-MLC), phosphorylated myosin light chain (p-MLC), MYPT1, phosphorylated MYPT1 (p-MYPT1), β-actin and all secondary antibodies were from Cell Signaling Technology (Boston, MA, USA). CFTR(inh)-172, Y27632, ML-7, Fura-2AM, RIPA Lysis Buffer (10X), protease inhibitor cocktail, L-nitro-arginine methyl ester (L-NAME), TritonX-100, EGTA, $MnCl_2$, pentobarbital sodium, Ang II, Hanks' Balanced Salt Solution (HBSS) and Krebs-Henseleit Modified Buffer were from were from Sigma Aldrich Corp. (St. Louis, MO, USA). Polyvinylidene difluoride (PVDF) membrane was from Millipore Corp. (Billerica, MA, USA). Pierce ECL substrate and sequence-specific primers were from Thermo Fisher Scientific (Waltham, MA, USA). Trizol reagent was from Invitrogen (Carlsbad, CA, USA), Transcriptor First Strand cDNA Synthesis Kit (Roche, Mannheim, Germany) and Fast start universal SYBR Green Master (ROX) were from Roche Molecular Biochemicals (Mannheim, BW, Germany). RhoA Activation Assay Kit was from Abcam (Cambridge, UK). Dulbecco's modified Essential medium/F-12 (DMEM/F12) medium, fetal calf serum were from Gibco (Carlsbad, CA, USA).

3.3 Cell isolation and culture

Basilar artery smooth muscle cells (BASMCs) were isolated from rat and mice basilar arteries as we previously described [22]. Briefly, 4 weeks old male Sprague–Dawley rats, 5–8 weeks old $Cftr^{+/+}$ and $Cftr^{-/-}$ mice were anesthetized with pentobarbital sodium (50 mg/kg, intraperitoneally). The basilar arteries were collected immediately and immersed in Krebs solution containing 10^5 U/L penicillin and 100 mg/L streptomycin. After the connective tissue was cleaned, the basilar arteries were cut into small pieces about 0.5 mm long and the vessel segments were placed on the surface of the dish. The dish was then incubated in DMEM/F12 supplemented with 20% fetal calf serum at 37 °C and 5% CO_2. Passages 4–6 of the cultured BASMCs were used for experiments.

3.4 Adenovirus transfection

Ad-*Cftr* and Ad-*Cftr*-shRNA were designed and produced by GENECHEM (Shanghai, CN). The cDNA of *Cftr* plasmid was a kind gift from Dr. Jim Hu (University of Toronto, ON, CA). The sequence of *Cftr* (NM_031506) shRNA was 5′-CCGGGCTGAAAGCAGGTGGGATTCTCAAGAGAAATCCCACCTGCTTTCAGCTTTTTTG-3′. Adenovirus was transfected using the protocol previously described [21]. Briefly, cultured BASMCs at 50% confluence were infected with adenovirus encoding *Cftr* or *Cftr* shRNA for 6 h in serum-free medium, and then cells were washed and incubated in fresh complete medium for another 48 h before harvested.

3.5 Western blot analysis

Western blot was performed as previously described [22]. Briefly, cells or tissues were lysed with RIPA

lysis buffer containing protease inhibitor cocktail. Protein was separated with 8% or 10% SDS-PAGE and transformed to a PVDF membrane. After blocked with 5% milk for 1 h at room temperature, the membrane was incubated with primary antibody at 4 °C overnight and then with secondary antibody for 1 h at room temperature. For analysis of CFTR expression in arteries or in VSMCs, proteins were extracted in lysis buffer and immunoblotted with anti-CFTR primary antibody (1:500, Alomone Labs) [23], and detected with HRP-linked secondary antibodies. Immunogen of CFTR antibody: Peptide (C) KEETEEEVQDTRL, corresponding to amino acid residues 1468–1480 of human CFTR (Accession P13569). Final band detection was performed with a Pierce ECL substrate by using a BIO-RAD molecular imager ChemiDoc XRS+ (Bio-Red, Hercules, CA). The densities of the target bands were determined by ImageJ software (National Institutes of Health, Bethesda, MD, USA).

3.6 Quantitative real time PCR

Quantitative real time PCR (qRT-PCR) was performed as previously described [24]. Briefly, the total RNA was extracted from basilar arteries using Trizol reagent according to the manufacturer's instructions. Purity and concentration of isolated total RNA were measured using the TECAN infinite M100 PRO Biotek microplate reader (Tecan Group, Ltd., Männedorf, Switzerland). First-strand cDNA was generated from 1 μg of total RNA using Transcriptor First Strand cDNA Synthesis Kit and qRT-PCR was performed using the Fast Start Universal SYBR Green Master (ROX) according to the manufacturer's instructions. The total reaction volume was 20 μL, including 10 μL of 2 $\times$ SYBR Green Master, 0.6 μL of PCR Forward Primer (10 μM), 0.6 μL of PCR Reverse Primer (10 μM), 2 μL of cDNA (20 ng) and 7 μL of double-distilled water. The qRT-PCR was set at an initial step of 10 min at 95 °C, followed by 40 cycles at 95 °C for 15 seconds and then 60 °C for 60 seconds. qRT-PCR was executed using iQ5 real-time PCR detection system (Bio-Rad Laboratories, Inc, CA, USA). All experiments were done in triplicate, and all samples were normalized to GAPDH. The expression levels were calculated using $2^{-\Delta\Delta Ct}$ methods. Melting curve analysis was performed in the range of 60 °C to 95 °C, 0.5 °C per 5 seconds increments. The sequence-specific primers were used as follows: CFTR, 5′-GGATGCTGAGGAAGCAACTC-3′ (forward) and 5′-CCAGCCTGGAACTCTCTTTG-3′ (reverse); GAPDH, 5′-AGGTCGGTGTGAACGGATTTG-3′ (forward) and 5′-TGTAGACCATG TAGTTGAGGTCA-3′ (reverse).

3.7 Isometric tension measurement in arteries

Vascular rings of thoracic aorta and basilar artery were prepared and isometric tension measurement experiments were performed as previously described [25]. Briefly, mice were euthanized and then thoracic aortas or basilar arteries were quickly removed and placed into ice-cold Krebs-Henseleit Modified Buffer containing 2.5 mM Ca^{2+} (Krebs buffer), and detached from fatty and connective tissues. Aortic ring segments (3–5 mm) and basilar artery ring segments (2 mm) were fixed on the Wire Myograph System (Danish Myo Technology, Denmark) and immersed in Krebs buffer aerated with 95% O_2/5% CO_2 and maintained at 37 °C. The rings were stretched to an optimal resting tension (3 mN) and allowed to stabilize for 1 h. 60 mM of KCl was used to stimulate vessel contraction for 3 times, the difference of isometric force should be less than 5% between each time. At the end of each stimulation, the original equilibrium tension of vessels were recovered after washed by Krebs buffer for 3 times. The vessels were then balanced for 30 min, followed by subsequent experiments. During the measurement process, endothelium of the arteries was chemically denudated by L-NAME (10 μM). Isometric force were recorded using PowerLab data acquisition system (AD Instruments Inc, US).

3.8 Intracellular Ca^{2+} concentration measurement

$[Ca^{2+}]_i$ was measured as we previously described [26]. Briefly, VSMCs were digested and incubated with DMEM/F12 medium containing 2 μM of Fura-2/AM for 45 min at 37 °C, then the cells were washed with HBSS buffer containing 2 mM Ca^{2+} 3 times and resuspended. The number of cells was adjusted to 10^6 cells per mL. Fluorescence emission was monitored at 500 nm using RF-5301 fluorescence Spectrophotometer (Shimadzu, Tokyo, Japan) with an excitation at 340 and 380 nm. $[Ca^{2+}]_i$ was determined from the formula: $[Ca^{2+}]_i$ = Kd $\times$ Sf380/b380(R–Rmin)/(Rmax–R), where Kd is 224 nm at 37 °C; Sf380/b380 is the ratio of the intensities of the free and bound dye forms at 380 nm; R is the fluorescence ratio (340 nm/380 nm) of the intracellular Fura-2/AM; Rmax and Rmin are the maximal and minimal fluorescence ratios obtained by addition of Triton X-100 (0.09%) and EGTA (3 mM) respectively. Ang II (100 nM) was added to the cell suspension when the fluorescence intensity was stable.

3.9 Measurements of Mn^{2+} quenching of fura-2 fluorescence

As we described previously [27], VSMCs were digested and incubated with 2 μM of Fura-2/AM for 45 min at 37 °C, then the cells were washed with HBSS buffer containing 1.3 mM Ca^{2+} 3 times and resuspended with Ca^{2+}-free HBSS buffer. The number of cells was adjusted to 10^6 cells per ml. After baseline fluorescence got to steady state, Mn^{2+} was injected into the cuvette with the final concentration of 500 μM. Fluorescence intensity was detected by RF-5301 Fluorescence Spectrophotometer (Shimadzu, Tokyo, Japan) with magnetic stirring at 37 °C. The excitation wavelength was 360 nm and the absorption wavelength was 510 nm. After the fluorescence value was relatively stable, Ang II were added to stimulate the flow of divalent cations.

3.10 RhoA activation assay

RhoA-GTP and total RhoA were detected using a RhoA Activation Assay Kit according to manufacturer's instruction. Briefly, the anti-active RhoA (RhoA-GTP) mouse monoclonal antibody was incubated with cell lysates. The bound RhoA-GTP was then pulled down by protein A/G agarose beads at 4 °C for 1 h. The beads were centrifuged and washed, and then boiled in SDS-PAGE sample buffer. Samples were resolved on 10% SDS-PAGE gels and transferred to PVDF membranes and incubated with anti-RhoA Rabbit polyclonal antibody. Total RhoA was detected by western blot of the cell lysates using anti-RhoA rabbit polyclonal antibody provided in the kit.

3.11 Statistics

All data are expressed as mean ± SEM with n representing the number of independent experiments on different batches of cells or different mice. All statistical analyses were performed using Prism 9 (GraphPad software, San Diego, CA). Student's *t* test (2-tailed) was used to detect significant differences between two groups while one-way ANOVA followed by Bonferroni multiple comparison test was used to compare differences between three groups or more. Values were considered statistically significant when $p < 0.05$.

4. Results

4.1 CFTR participates in the progress of Ang II induced hypertension

Ang II of various infusion rates (125, 250, 500 and 1000 ng/kg/min) was administrated to *Cftr*$^{+/+}$ mice using osmotic pumps for 14 days. In comparison to sham group, mice administrated with 500 and 1000 ng/kg/min Ang II exhibited significant higher systolic blood pressure (SBP), which were 139.33 ± 2.58 and 159.67 ± 4.57 mmHg (Fig. 1A). Meanwhile, *Cftr* mRNA level in basilar arteries was significantly reduced in these two groups (Fig. 1B) and negative correlation between *Cftr* mRNA and SBP was observed (Fig. 1C). Moreover, CFTR protein expression was decreased in basilar arteries from Ang II induced hypertensive rats (Fig. 1D). These *in vivo* data suggested that arterial CFTR was downregulated only if SBP was elevated.

In previous study, average SBP and DBP of 24-hour, daytime and night time of *Cftr*$^{-/-}$ mice were all significantly higher than those of *Cftr*$^{+/+}$ mice, however, *Cftr* knockout did not alter SBP or DBP recorded from 4:00 PM to 8:00 PM [12]. To investigate whether CFTR play a part in Ang II induced hypertension, *Cftr*$^{+/+}$ and *Cftr*$^{-/-}$ mice were used to establish Ang II infusion induced hypertension model, SBP and DBP was measured at 6:00 PM 0, 3, 6, 9, 12 and 14 days after the pumps were implanted. We found that SBP of *Cftr*$^{-/-}$ mice was significantly higher than that of *Cftr*$^{+/+}$ mice since day 6 (Fig. 1G). DBP was also additionally increased in *Cftr*$^{-/-}$ mice on day 3, 12, and 14 (Fig. 1H). Baseline SBP and DBP of *Cftr*$^{+/+}$, *Cftr*$^{+/-}$ and *Cftr*$^{-/-}$ mice were also measured at 6:00 PM, as shown in **Supplementary Fig. 1**, *Cftr* knockout did not affect BP in physiological state. These *in vivo* data indicated that *Cftr* knockout aggravated Ang II induced hypertension.

4.2 Cftr knockout or pharmacological inhibition enhanced vasoconstriction in response to Ang II

In both sham and Ang II induced hypertensive mice, Ang II induced tension of thoracic aorta was significantly higher in *Cftr*$^{-/-}$ mice vs. *Cftr*$^{+/+}$ mice (Fig. 2A,B). Furthermore, preincubation of CFTR specific inhibitor CFTR(inh)-172 (5 μM) for 5 min significantly increased Ang II induced vasoconstriction in thoracic aorta and basilar artery, which were isolated from *Cftr*$^{+/+}$ mice and SD rats, respectively (Fig. 2C,D). Additionally, KCl induced arterial tension was also enhanced by CFTR(inh)-172 (Fig. 2E), while no significant effect could be observed when thromboxane analogue U46619, 5-HT, or phenylephrine were used as stimulators (Fig. 2F–H). These data demonstrated that short-term pharmacological or genetic inhibition of CFTR increased vasoconstriction in response to Ang II in both normotensive and hypertensive arteries.

4.3 Effect of CFTR on the phosphorylation of MLC in VSMCs *in vivo* and *in vitro*

The reversible phosphorylation of regulatory myosin light chain (MLC) is the core of VSMCs contraction. To investigate the effect of CFTR on MLC phosphorylation *in vivo*, *Cftr*$^{+/+}$ and *Cftr*$^{-/-}$ mice were used to establish Ang II infusion induced hypertension model, and the phosphorylated MLC (p-MLC) and total MLC (t-MLC) were detected. As shown in Fig. 3A, p-MLC in thoracic aortas was increased by Ang II infusion, and significantly higher in *Cftr*$^{-/-}$ mice in comparison to *Cftr*$^{+/+}$ ones in the hypertension group. No significant alteration was observed in t-MLC level (Fig. 3B). *In vitro*, CFTR overexpression adenovirus (Ad-*Cftr*), CFTR shRNA silencing adenovirus (Ad-*Cftr*-shRNA) and CFTR specific inhibitor CFTR(inh)-172 were used to alter the expression or activity of CFTR. As shown in Fig. 3C,D, p-MLC in primarily isolated basilar artery smooth muscle cells (BASMCs) was decreased by CFTR overexpression and increased by CFTR silencing or CFTR(inh)-172 incubation for 48 h, while no significant alteration was observed in t-MLC level (**Supplementary Fig. 1**). These data demonstrated that both CFTR expression and long-term activity inhibition could affect MLC phosphorylation level in resting VSMCs.

4.4 Effect of CFTR on Ang II induced Ca^{2+} influx in VSMCs

Cytosolic Ca^{2+} concentration elevation is a trigger for vascular contraction. A defect in the regulation of Ca^{2+} signaling plays a role in hypertension associated vascular dysfunction. For smooth muscle cell contraction to occur,

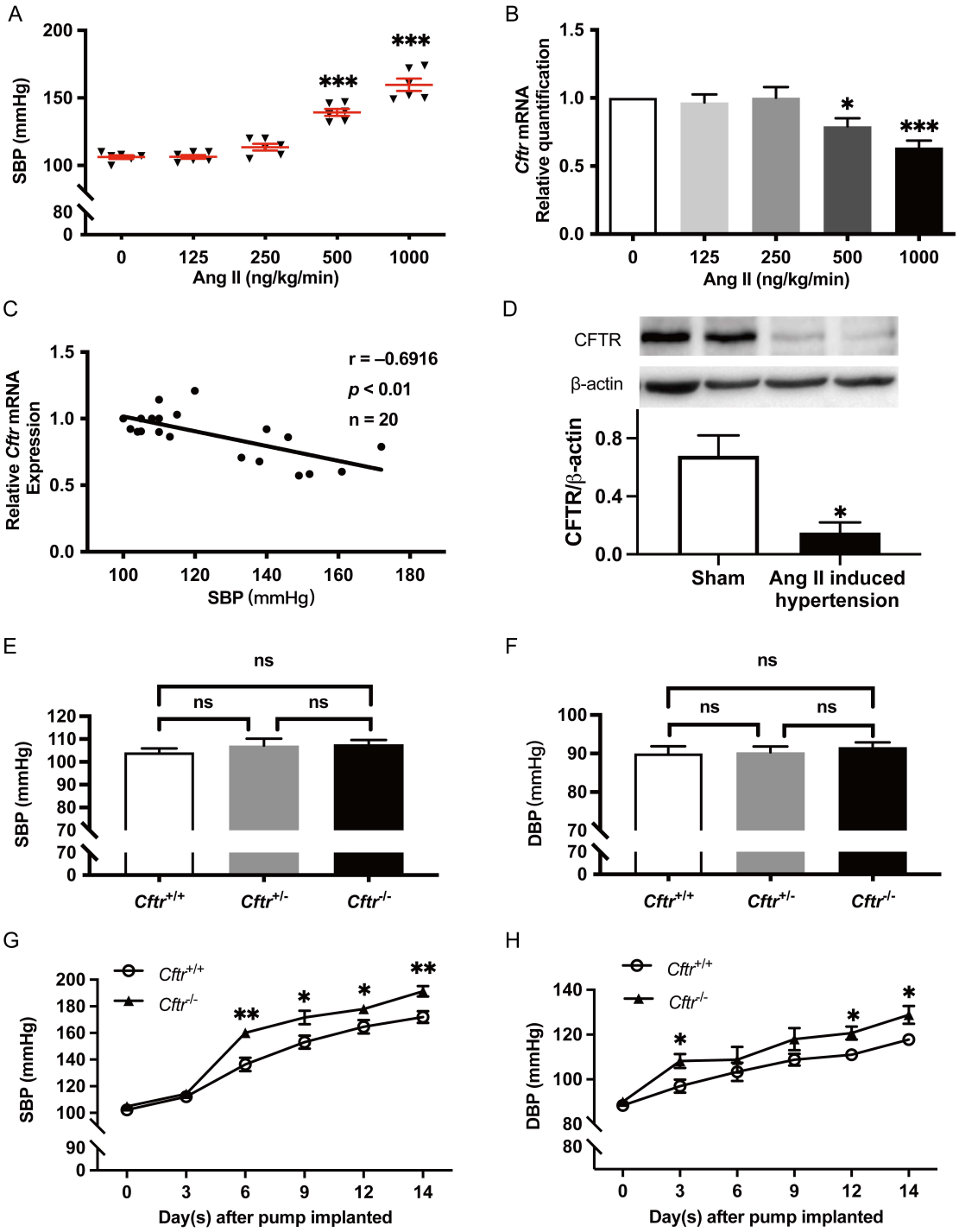

Fig. 1. Expression of CFTR is downregulated in hypertensive arteries and *Cftr* knockout enhanced Ang II induced blood pressure elevation. (A) Ang II of 0, 125, 250, 500 and 1000 ng/kg/min was administrated for 14 days to obtain Ang II induced hypertensive mice model. Systolic blood pressure (SBP) was significantly elevated in 500 and 1000 ng/kg/min groups. (B) *Cftr* mRNA level in basilar arteries was also significantly reduced in 500 and 1000 ng/kg/min groups (n = 6, $*p < 0.05$ and $***p < 0.001$ vs. 0 ng/kg/min group). (C) Correlation analysis of basilar artery *Cftr* mRNA expression and SBP in Ang II induced hypertensive mice. (D) CFTR protein expression in basilar arteries was reduced in Ang II induced hypertensive rats (n = 6, $*p <$ 0.05 vs. Sham group). (E,F) No significant difference was observed in baseline SBP and DBP levels between $Cftr^{+/+}$, $Cftr^{+/-}$ and $Cftr^{-/-}$ mice (n = 6). (G,H) $Cftr^{+/+}$ and $Cftr^{-/-}$ mice were used to establish Ang II induced hypertensive model, SBP and DBP were measured 0, 3, 6, 9, 12, 14 days after 1000 ng/kg/min of Ang II infusion operation. In comparison to $Cftr^{+/+}$ mice, SBP and DBP measured in $Cftr^{-/-}$ mice were increased (n = 7–8, $*p < 0.05$ and $**p < 0.01$ vs. $Cftr^{+/+}$ group).

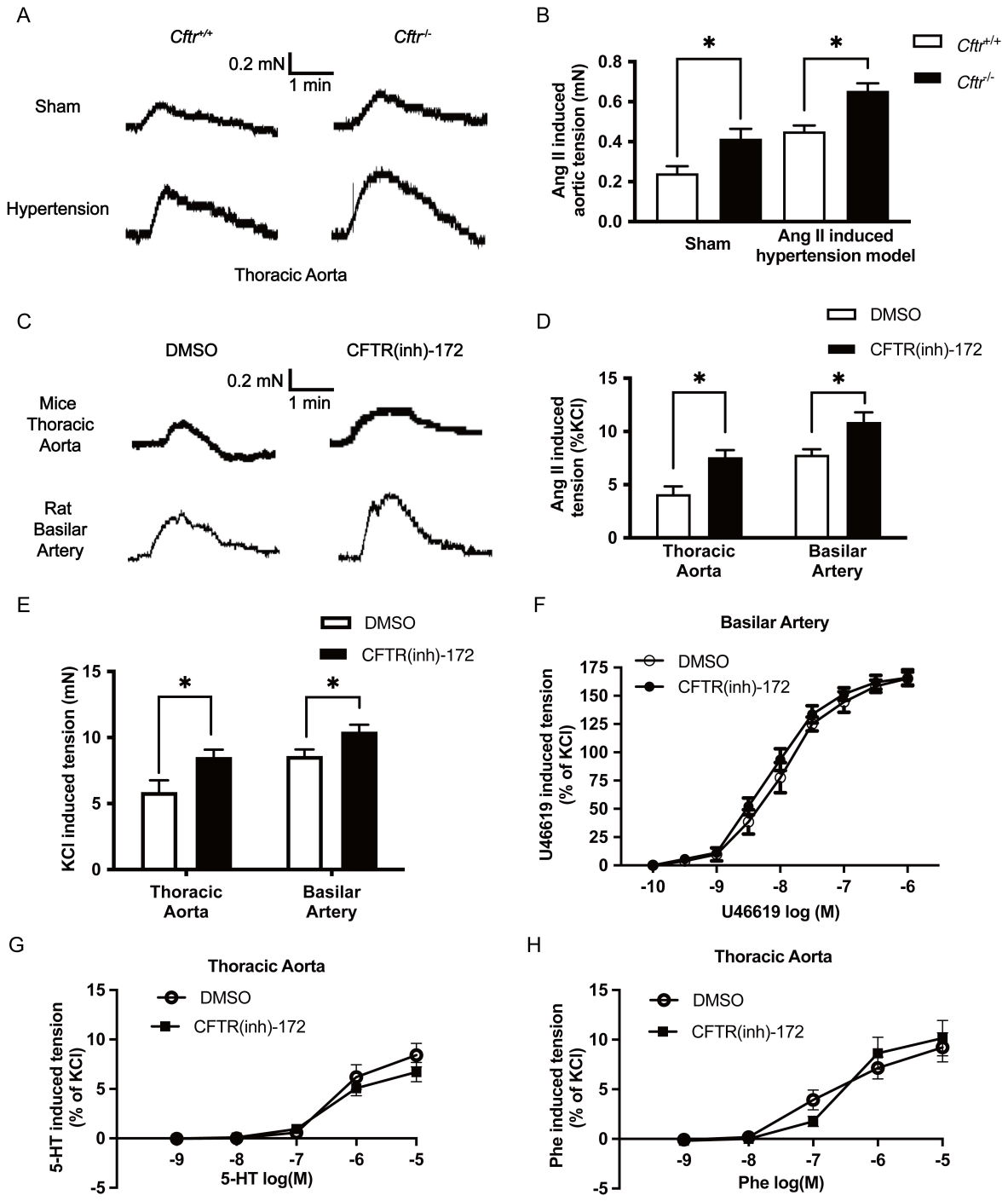

Fig. 2. Effect of *Cftr* knockout or pharmacological inhibition on vasoconstriction in response to different stimulus. (A–B) $Cftr^{+/+}$ and $Cftr^{-/-}$ mice were used to establish Ang II infusion induced hypertensive model and thoracic aortas were isolated. Endothelium of the vessel was chemically denudated by L-NAME (10 μM). Representative tracings of isometric tension in response to Ang II (1 μM) in thoracic aorta were shown. Maximum tension was adopted for analysis (n = 5–6, $*p < 0.05$). (C,D) Thoracic aortas and basilar arteries were isolated from C57BL/6J mice and SD rats, respectively, and conducted endothelial denudation. CFTR was pharmacologically inhibited by 5 min of preincubation with CFTR(inh)-172 (5 μM), while DMSO was used as solvent control. Arterial rings were incubated with Ang II (1 μM) for 5 min and representative tracings of isometric tension were shown. Ang II induced tension was expressed in the percentage of KCl (60 mM) induced tension in the absence of CFTR(inh)-172 (n = 6, $*p < 0.05$). (E) Arteries were pretreated with CFTR(inh)-172 (5 μM) for 5 min and KCl (60 mM) induced tension were measured (n = 8, $*p < 0.05$). (F–H) Concentration-response curves of U46619, 5-HT and phenylephrine (Phe) were drawn in the presence or absence of CFTR(inh)-172, no significant difference in tension could be observed (n = 5).

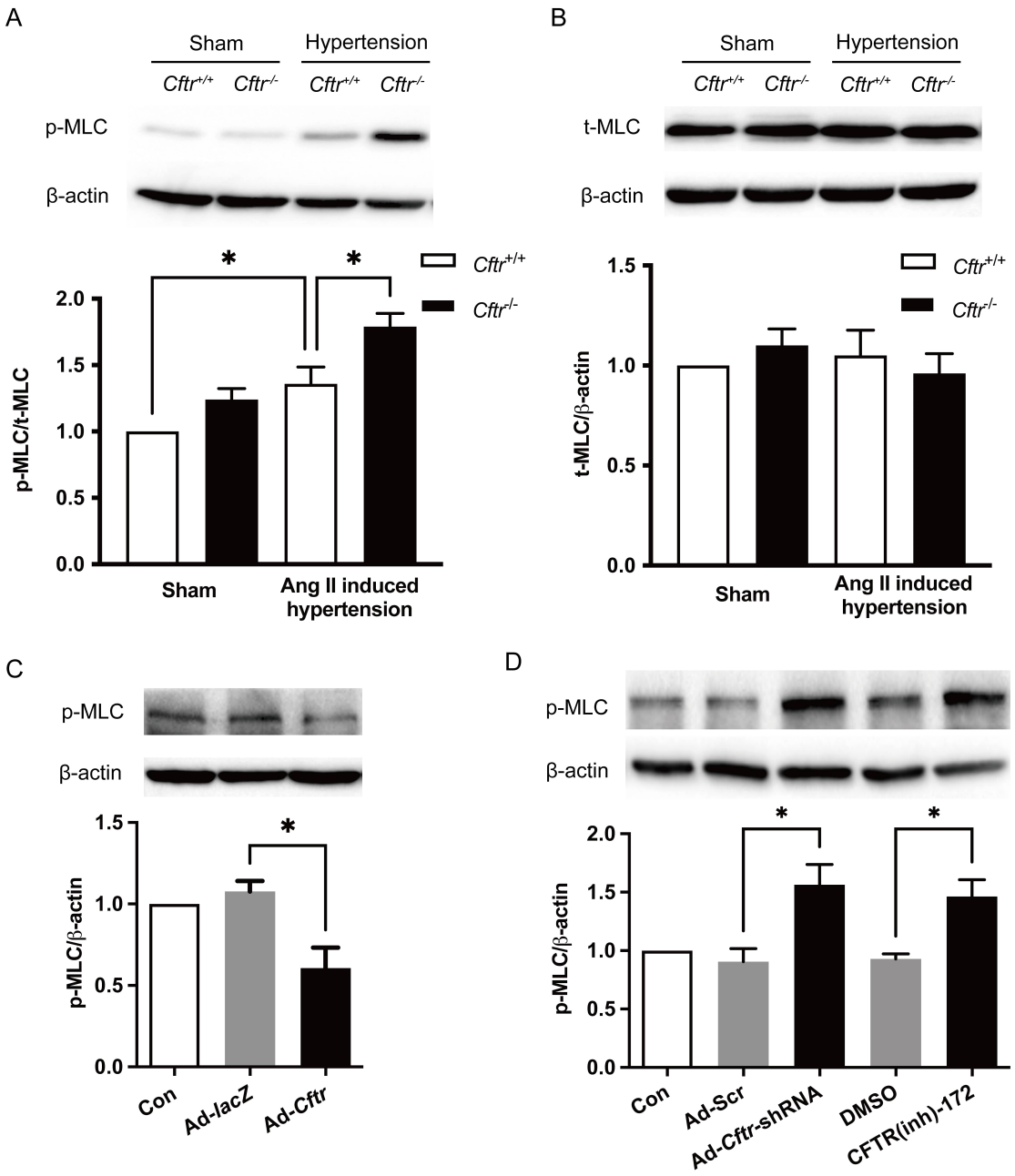

Fig. 3. Downregulation/inhibition of CFTR increased the phosphorylation level of myosin light chain *in vivo* and *in vitro*. (A,B) $Cftr^{+/+}$ and $Cftr^{-/-}$ mice were used to establish Ang II infusion induced hypertensive model. Thoracic aortas were isolated from hypertensive group and sham group, phosphorylated myosin light chain (p-MLC) and total myosin light chain (t-MLC) were detected by western blot (n = 6 mice, $*p < 0.05$). *Cftr* knockout increased p-MLC in Ang II induced hypertensive arteries. (C,D) p-MLC level in basilar artery smooth muscle cells (BASMCs) were measured with CFTR overexpression, silencing or pharmacological inhibition. Ad-*Cftr*, Ad-*Cftr*-shRNA or CFTR(inh)-172 (5 μM, 48 h) were used, respectively. BASMCs were treated with Ad-*Cftr* or Ad-*Cftr*-shRNA for 6 h followed by cultivation with DMEM/F12 medium containing 10% FBS for another 48 h. Ad-*lacZ* and Ad-Scr were used as negative control, respectively. p-MLC (C,D) and t-MLC (see in **Supplementary Fig. 1**) in cell lysates were detected by western blot (n = 6, $*p < 0.05$).

cytosolic Ca^{2+} binds to calmodulin, and Ca^{2+}/calmodulin complex interacts with MLC, leading to the activation of MLCK and phosphorylation of MLC. To investigate whether CFTR works through Ca^{2+}-dependent pathway, effect of CFTR on Ang II induced increase in $[Ca^{2+}]_i$ was detected. BASMCs were cultured from $Cftr^{+/+}$ or $Cftr^{-/-}$ mice, and CFTR overexpression in $Cftr^{+/+}$ BASMCs was conducted using Ad-*Cftr*. 100 nM of Ang II was added to stimulate $[Ca^{2+}]_i$ increase with 2 mM of extracellular Ca^{2+}. As shown in Fig. 4A,C, CFTR did not affect basal $[Ca^{2+}]_i$ in resting BASMCs, however, BASMCs from $Cftr^{-/-}$ mice exhibited higher $[Ca^{2+}]_i$ in response to

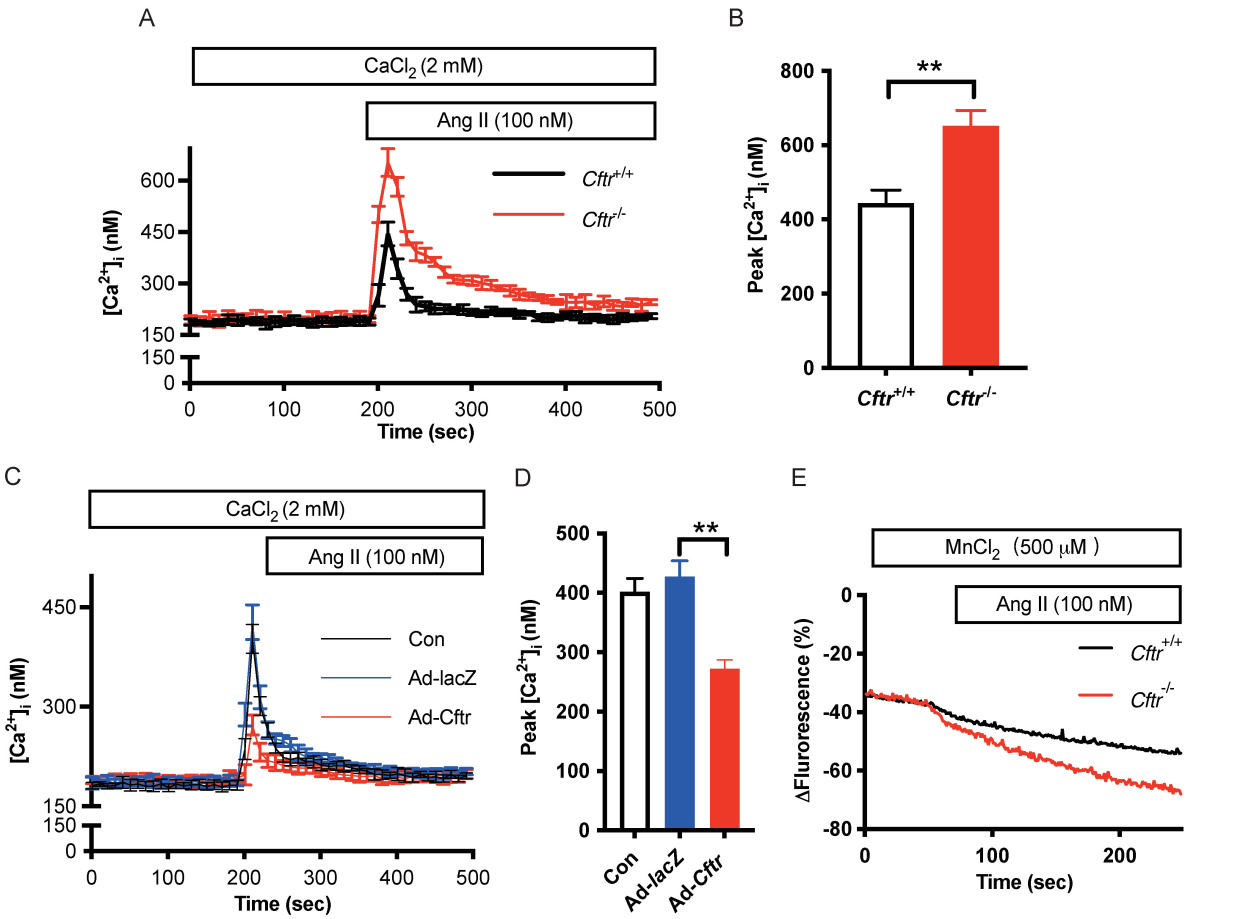

Fig. 4. Effect of CFTR on Ang II induced Ca^{2+} influx in cultured BASMCs. (A) BASMCs were isolated from *Cftr*$^{+/+}$ and *Cftr*$^{-/-}$ mice and cultured in DMEM/F12 medium with 20% FBS. Intracellular calcium concentration ($[Ca^{2+}]_i$) was monitored and recorded every 10 seconds with 2 mM of extracellular Ca^{2+}. Ang II (100 nM) was added after the fluorescence was stable. (B) Maximum of $[Ca^{2+}]_i$ in response to Ang II were compared between BASMCs from *Cftr*$^{+/+}$ and *Cftr*$^{-/-}$ mice (n = 6, $^{**}p < 0.01$). (C) BASMCs were treated with Ad-*lacZ* (100 MOI) or Ad-*Cftr* (100 MOI) for 6 h followed by cultivation with DMEM/F12 medium containing 10% FBS for another 48 h. $[Ca^{2+}]_i$ was monitored and recorded every 10 seconds with 2 mM of extracellular calcium concentration. Ang II (100 nM) was added after the fluorescence was stable. (D) Maximum of Ang II induced $[Ca^{2+}]_i$ rise were compared between Ad-*lacZ* and Ad-*Cftr* group. (n = 6, $^{**}p < 0.01$). (E) Measurement of Mn^{2+} quenching rate. BASMCs were cultured from *Cftr*$^{+/+}$ and *Cftr*$^{-/-}$ mice, digested and incubated with 2 μM Fura-2AM for 45 min and then washed and resuspended with Ca^{2+} free HBSS. Fluorescence in response to Ang II was recorded every second. Quenching rate was expressed as percentage change of the maximum rate.

Ang II compared to that from *Cftr*$^{+/+}$ mice (Fig. 4B), while CFTR overexpression caused a decrease in Ang II induced $[Ca^{2+}]_i$ rise (Fig. 4D). Then we went further for the Mn^{2+} quenching rate measurement and found that *Cftr* knockout also enhanced Ang II induced Mn^{2+} influx (Fig. 4E). These results for the first time demonstrated that CFTR was involved in Ang II induced Ca^{2+} influx, and thus initiated MLCK activation and the consequent MLC phosphorylation.

4.5 Regulating effect of CFTR on the phosphorylation of MYPT1 via RhoA/Rock pathway

As shown in Fig. 3C,D,4A,C, in resting VSMCs, CFTR could regulate the phosphorylation of MLC without affecting resting $[Ca^{2+}]_i$. In addition, CFTR overexpression did not alter MLCK protein expression level (Fig. 5A), and with MLCK activity inhibited by ML-7, CFTR overexpression could still decrease p-MLC (Fig. 5B), suggesting that CFTR might regulate resting tension of VSMCs through Ca^{2+}-independent pathway.

While MLCK-mediated constriction is strictly dependent on $[Ca^{2+}]_i$, MLC phosphorylation and the subsequent constriction can be maintained even after $[Ca^{2+}]_i$ returns to basal levels via inhibition MLCP. MLCP holoenzyme consists of three subunits: catalytic subunit of protein phosphatase 1 (PP1), myosin phosphatase target subunit 1 (MYPT1) and a subunit of unknown function [28]. The binding of MYPT1 to PP1 unit increases MLCP catalytic activity, while phosphorylated MYPT1 (p-MYPT1) represses the catalytic activity of MLCP and thus enhances MLC phosphorylation and VSMCs contraction. p-MYPT1 is modulated by RhoA/ROCK pathway, which can be activated by various stimuli, including Ang II.

As shown in Fig. 5C–F, CFTR affected p-MYPT1 at site Thr855, but not at Ser507 or Thr696 in BASMCs. Incubation with selective Rock inhibitor Y-27632 decreased p-MYPT1 in resting BASMCs and abolished the enhancement of p-MYPT1 induced by long-term CFTR activity inhibition (48 h) (Fig. 5G), while CFTR overexpression decreased RhoA activation in resting and Ang II stimulated BASMCs (Fig. 5H). These data indicated that RhoA/Rock mediated MYPT1 phosphorylation might be another signaling pathway involved in the regulating effect of CFTR on vasoconstriction and thus hypertension. Our finding is in agreement with a previous report demonstrating that continuous inhibition CFTR-Cl^- conductance for 3–5 days resulted in a threefold increase in RhoA expression [29].

5. Discussion

Both human and murine studies suggest the *Cftr* mutation is associated with blood pressure and vascular dysfunction, however, the role of CFTR in the genesis of hypertension remains quite unillustrated. In the present study, we provided the first piece of evidence that *Cftr* participated in the progression of Ang II induced hypertension. Our findings are as follows: (1) *Cftr* knockout enhanced BP elevation in Ang II infusion induced hypertensive mice, while CFTR mRNA/protein expression were decreased in hypertensive arteries. (2) Both genetic and pharmacological inhibition of CFTR increased Ang II induced vasoconstriction and the phosphorylation of MLC in VSMCs. (3) $[Ca^{2+}]_i$ rise induced by Ang II in VSMCs was increased by *Cftr* knockout and decreased by CFTR overexpression, while basal $[Ca^{2+}]_i$ was not affected by CFTR in resting VSMCs. (4) CFTR regulated the phosphorylation of MYPT1 at site Thr855 via RhoA/Rock pathway in both resting and Ang II stimulated VSMCs.

CFTR has been studied in cardiovascular system, including left ventricular remodeling [30], elevated myocardial contractility [31], cardio-protection against acidosis/ischemia [32] and cardiac development during early embryogenesis [33]. CFTR is a cAMP-dependent Cl^- channel best known for its role in Cl^- and $HCO_3{}^-$ transport in epithelial tissues [34]. Older female CF mutation (not gene deletion) carriers showed lower BP than matched control subjects [11] and F508del heterozygous mice had lower arterial pressures than wild-type mice [35], which had been attributed to excessive salt depletion. Ya-Ping Zhang *et al.* [12] demonstrated that 24-hour average physiological SBP and DBP of $Cftr^{-/-}$ mice were all significantly higher than those of $Cftr^{+/+}$ mice.

It is noteworthy that previous studies only mentioned the relationship between physiological BP and CFTR, however, the effect of CFTR on pathophysiological BP level in the process of hypertension remains unillustrated. In the present study, we established the Ang II infusion induced hypertension model and found that CFTR expression in hypertensive arteries were decreased and negatively related with BP level. Moreover, *Cftr* knockout enhanced Ang II induced BP elevation during the development of hypertension, without altering BP in normotensive mice. Previous study indicated that CFTR might play a little role in circadian regulation of BP [12]. Both $Cftr^{-/-}$ and $Cftr^{+/+}$ mice displayed a bimodal circadian pattern over 24-hour period but BP peaks of $Cftr^{-/-}$ mice were higher and later when compared to $Cftr^{+/+}$ mice. As a result of this regulatory effect, *Cftr* knockout did not alter SBP or DBP measured from 4:00 PM to 8:00 PM. Because the aim of our study was to investigate the role of CFTR in the development of hypertension, all BP values recorded in our study was measured at 6:00 PM of the day, avoiding the influence of the *Cftr* knockout on physiological BP.

The effect of *Cftr* mutation on blood pressure in previous studies had been attributed to excessive salt depletion or absorption [11, 35, 36], however, hypertension is pathologically characterized by augmented vascular contractility and chloride channels in VSMCs have been identified as important regulators of vascular tone. As a small outwardly rectifying chloride channel, the effect of CFTR on vasoconstriction should get more attention. In previous studies, aortic diameter measured at valsalva sinuses was significantly higher in patients with CF mutations [37]. CFTR inhibition enhanced pressure-induced myogenic vasoconstriction [15], and aortic rings from $Cftr^{-/-}$ mice showed a much stronger depolarization induced vasoconstriction than those from wild-type mice [16]. In addition, the loss of CFTR function (F508del) enhanced posterior cerebral arteries myogenic vasoconstriction in response to phenylephrine, while CFTR corrector compounds normalize pathological alterations in cerebral artery CFTR expression, vascular reactivity, and cerebral perfusion [18]. Conversely, aortas from piglets with F508del mutation showed decreased vascular tone in response to 60 mM of KCl, while no difference was observed in CFTR null piglets [38]. Regulating effect of CFTR on vasoconstriction remains controversial. In this study, we demonstrated that *Cftr* knockout enhanced Ang II induced constriction of thoracic aortas in both Sham and Ang II induced hypertensive mice. In addition, short-term inhibition of CFTR channel activity by CFTR(inh)-172 increased vascular tension in response to Ang II in both thoracic aortas and basilar arteries. These results were consistent with the data of blood pressure we observed in Ang II induced hypertensive $Cftr^{-/-}$ mice. Notably, phenylephrine, 5-HT and U46619 can cause adenylate cyclase (AC) activation and the production of cAMP [39], which can activate CFTR channel. Therefore, it is conceivable that phenylephrine, 5-HT or U46619 induced arterial tension was not altered by short-term CFTR activity inhibition, which might be due to the counterbalance of cAMP and CFTR(inh)-172.

Growing evidence indicates that Ca^{2+} signaling and CFTR are interdependent. Binding of CFTR to iso-

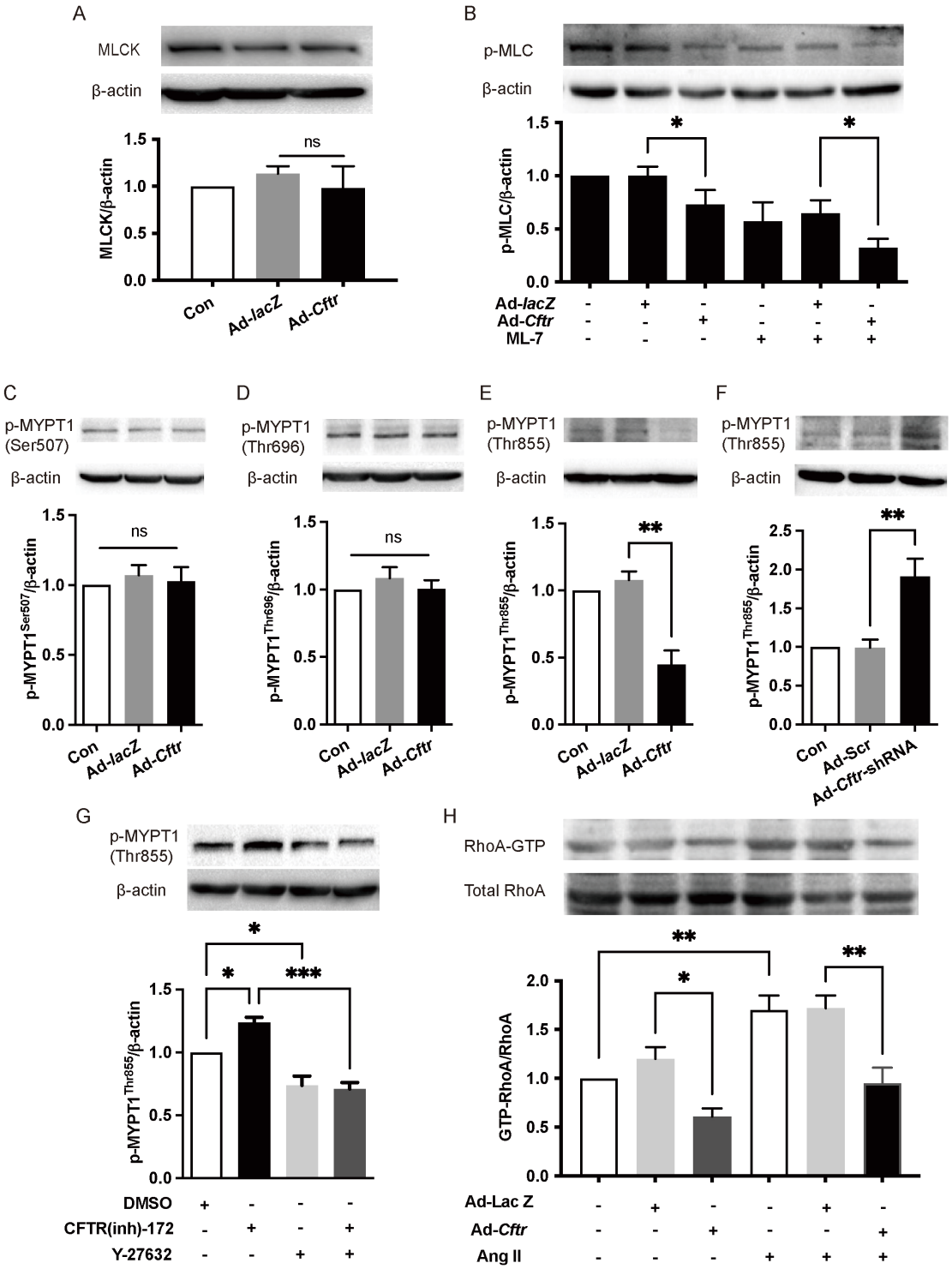

Fig. 5. Effect of CFTR on phosphorylation of MYPT1 via adjusting RhoA activity. (A) BASMCs were treated with Ad-*Cftr* or Ad-*lacZ* for 6 h and cultured with 10% FBS DMEM/F12 medium for another 48 h. MLCK expression was detected by western blot and no significant difference was observed (n = 6). (B) ML-7 (inhibitor of MLCK, 10 μM) was applied during the whole process of CFTR overexpression treatment in BASMCs. Cell lysates were collected and p-MLC was detected by western blot (n = 6, *$p < 0.05$). (C–F) BASMCs were treated with Ad-*Cftr*, Ad-*Cftr*-shRNA or negative control vector for 6 h and cultured with DMEM/F12 medium with 10% FBS for another 48 h. Cell lysates were collected and MYPT1 phosphorylation at Ser507, Thr696 and Thr855 and total MYPT1 expression were detected using western blot (see in **Supplementary Fig. 2**), β-actin was used as loading control. (n = 6, **$p < 0.01$). (G) BASMCs were treated with CFTR(inh)-172 (5 μM, 48 h) and/or Y-27632 (10 μM, 48 h) and terminated by liquid nitrogen. Cell lysates were collected and p-MYPT1^{Thr855} was detected by western blot (n = 6, *$p < 0.05$, ***$p < 0.001$). (H) BASMCs were treated with Ad-*Cftr* or Ad-*lacZ*, Ang II (100 nM) was added for 5 min to induce cell contraction and then liquid nitrogen was used to terminate the process immediately. Cell lysates were collected and RhoA-GTP and total RhoA were detected using RhoA Activation Assay Kit (n = 6, *$p < 0.05$, **$p < 0.01$).

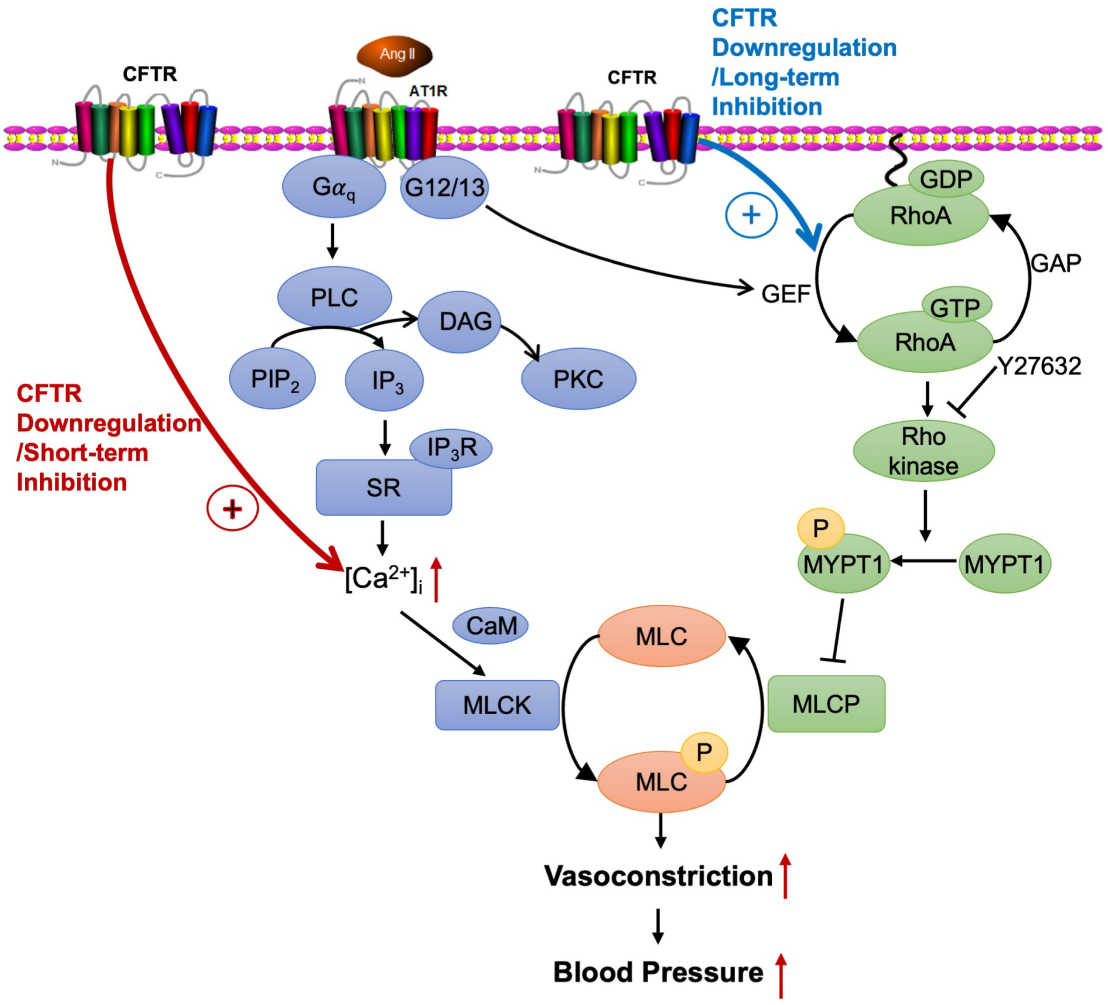

Fig. 6. Summary of the mechanisms underlying the regulating effect of CFTR on vasoconstriction. In VSMCs, Ang II binding to AT_1R regulates contraction through $G_{q/11}$ Ca^{2+}-sensitive MLCK activation and $G_{12/13}$ Rho/Rho kinase-mediated inhibition of MLC phosphatase (MLCP). Production of arachidonic acid derived hydroxyeicosatetraenoic acids (HETEs) and formation of NADPH oxidase-derived reactive oxygen species (ROS) were also involved in Ang II/AT1R mediated vasoconstriction. Activation of AT1 receptor by Ang II in VSMCs results in PLC activation leading to the release of the second messengers IP_3 and DAG. Activation of IP_3R stimulates intracellular Ca^{2+} release from sarcoplasmic reticulum and DAG causes PKC activation. Different Ca^{2+} entry channels, such as voltage-dependent, receptor-operated, and store-operated Ca^{2+} channels are involved in the elevation of intracellular Ca^{2+} concentration. The elevation in $[Ca^{2+}]_i$ initiates contractile activity by a Ca^{2+}-CaM interaction, causing MLCK activation and consequent MLC phosphorylation, which in turn enables the interaction between myosin and actin and initiates VSMCs contraction. In the absence of significant increase in $[Ca^{2+}]_i$, MLC phosphorylation can still be induced by pathway mediated by RhoA, which switches between an inactive GDP-bound state and an active GTP-bound state in response to various stimuli, including Ang II. RhoA activation induces phosphorylation of MYPT1, which inhibits the dephosphorylation of MLCP and thereby maintains force generation. In Ang II stimulated VSMCs, CFTR down-regulation and short-term inhibition increased Ca^{2+} influx and the subsequent MLC phosphorylation, besides, RhoA/Rock mediated MLCP inactivation could also be involved. In resting VSMCs, CFTR down-regulation or long-term inhibition increased MLC phosphorylation by affecting RhoA mediated MYPT1 phosphorylation.

lated calmodulin activated CFTR independent of protein kinase A (PKA) [40], and CFTR was necessary for forskolin induced $[Ca^{2+}]_i$ response in human airway epithelia [41]. Endoplasmic reticulum (ER) localized F508del-CFTR affected store-operated calcium channel (SOCC) Orai1 function and strongly enhanced calcium signaling in nasal epithelial cells [42, 43]. Our data further revealed that CFTR modulated Ang II induced Ca^{2+} influx in VSMCs. However, it has not been clarified in this work that how CFTR modulated the influx of Ca^{2+} in Ang II-stimulated VSMCs. SOCC, voltage-dependent Ca^{2+} channels, CaM-CFTR complex and all other pathways mediating the rise of $[Ca^{2+}]_i$ in response to Ang II might be involved in this process, further investigation is required in the future.

In resting VSMCs, CFTR did not alter basal $[Ca^{2+}]_i$ but regulated MLC phosphorylation even with MLCK activity inhibited, suggesting that Ca^{2+}-dependent MLC phosphorylation through MLCK cannot explain all

modalities of the effect of CFTR in arterial contraction. It was reported that CFTR disruption induced an increase in baseline myocardial contractility *in vivo*, in the absence of changes in the magnitude of Ca^{2+} transients [31]. Thus, we speculate that there might be different mechanisms underlying the regulating effect of CFTR on VSMCs contraction in resting and contractile states. As mentioned above, phosphorylation of MLC is controlled by a balance in the activity of MLCK and myosin MLCP and RhoA/Rock pathway regulates MLCP via phosphorylating its regulatory subunit MYPT-1 [44]. We found that selective Rock inhibitor Y-27632 decreased MYPT1 phosphorylation, and CFTR silencing increased RhoA activation, in both resting and Ang II stimulated BASMCs. Our results are in agreement with a previous report demonstrating that continuous inhibition CFTR-Cl^- conductance for 3–5 days resulted in a three-fold increase in RhoA expression [29], the effect of long-term inhibition of CFTR channel activity might be due to the augmented RhoA activation caused by the increased intracellular chloride concentration $[Cl^-]_i$ [45]. Based on these findings, we considered two possible mechanisms accounting for the regulation of CFTR on vasoconstriction of VSMCs: in resting VSMCs, CFTR altered MLC phosphorylation through RhoA/Rock pathway, while in Ang II stimulated VSMCs, the modulation was conducted via both Ca^{2+} influx and RhoA/Rock mediated pathway.

In general, as the graphical summary shown in Fig. 6, both chloride channel activity and protein expression of CFTR are involved in vasoconstriction and Ang II induced hypertension. Pharmacological inhibition of CFTR activity (short-term, pre-incubation for 5 min) enhanced Ang II induced artery constriction, but not resting arterial tension, while long-term inhibition (48 h) increased MLC and MYPT1 phosphorylation in VSMCs. CFTR protein expression level affected Ang II induced Ca^{2+} influx, RhoA activity, MYPT1, MLC phosphorylation and Ang II induced VSMC contraction and hypertension. Cl^- equilibrium potential is normally above the resting membrane potential in VSMCs [46]. Opening of Cl^- channels in the plasma membrane of VSMCs causes a Cl^- efflux, membrane depolarization, and increased contractile force. For instance, TMEM16A chloride channel promotes cell contraction and myogenic tone in different vascular beds [47–50]. Conversely, in our study, suppression of CFTR expression or activity enhanced Ang II stimulated vasoconstriction, indicating loss of active CFTR may have other consequences in addition to impairing Cl^- transport. For example, as a membrane protein, CFTR might directly interact with the upstream signaling molecule of Ca^{2+} or RhoA during the vasoconstriction process.

6. Conclusions

The present study demonstrated the critical role of CFTR in the genesis of Ang II induced hypertension. We showed for the first time that genetic ablation of *Cftr* aggravated elevation of BP in Ang II induced hypertensive mice. Both pharmacological and genetic inhibition of CFTR enhanced Ang II induced vasoconstriction, which was associated with Ca^{2+}-dependent signaling pathway and RhoA/Rock mediated phosphorylation of MYPT1. Our findings indicated that modification of CFTR might be a novel therapeutic strategy for hypertension.

7. Author contributions

LZ and GW designed the experiments; LZ, FY, NP, YY, HY, YL and RW conducted the experiments; LZ and FY analyzed the data; GW conceived and supervised the project; LZ drafted the manuscript; BZ and GW participated in data analysis and finalized the manuscript writing.

8. Ethics approval and consent to participate

All animal care and experimental procedures complied with the policies of Ethics Committee of ZSSOM on Laboratory Animal Care (approval number: 2016-080) and conformed to the “Guide for the Care and Use of Laboratory Animals” of the National Institute of Health in China.

9. Acknowledgement

Thanks to all the peer reviewers for their opinions and suggestions.

10. Funding

This study was supported by National Natural Science Foundation of China (81903687, 62172452, 82073848 and 81773722), Natural Science Foundation of Guangdong Province (2020A1515010045, China), Guangdong Provincial Department of Science and Technology (2017A020215104, China), the Science and Technology Program of Guangzhou City (201803010092, China).

11. Conflict of interest

The authors declare no conflict of interest.

12. References

[1] Forrester SJ, Booz GW, Sigmund CD, Coffman TM, Kawai T, Rizzo V, *et al*. Angiotensin II Signal Transduction: an Update on Mechanisms of Physiology and Pathophysiology. Physiological Reviews. 2018; 98: 1627–1738.

[2] Rattan S. Ca2+/calmodulin/MLCK pathway initiates, and RhoA/ROCK maintains, the internal anal sphincter smooth muscle tone. American Journal of Physiology. Gastrointestinal and Liver Physiology. 2017; 312: G63–G66.

[3] Bulley S, Jaggar JH. Cl^- channels in smooth muscle cells. Pflugers Archiv. 2014; 466: 861–872.

[4] McCallum L, Lip S, Padmanabhan S. The hidden hand of chloride in hypertension. Pflugers Archiv. 2015; 467: 595–603.

[5] Wang G, Wang X, Lin M, He H, Lan X, Guan Y. Deficiency in ClC-3 chloride channels prevents rat aortic smooth muscle cell proliferation. Circulation Research. 2002; 91: E28–E32.

[6] Guan Y, Wang G, Zhou J. The ClC-3 Cl− channel in cell volume regulation, proliferation and apoptosis in vascular smooth muscle cells. Trends in Pharmacological Sciences. 2006; 27: 290–296.

[7] Liu Y, Wang X, Tang Y, Chen J, Lv X, Zhou J, *et al*. Simvastatin ameliorates rat cerebrovascular remodeling during hypertension via inhibition of volume-regulated chloride channel. Hypertension. 2010; 56: 445–452.

[8] Zheng L, Li L, Ma M, Liu Y, Wang G, Tang Y, *et al*. Deficiency of volume-regulated ClC-3 chloride channel attenuates cerebrovascular remodelling in DOCA-salt hypertension. Cardiovascular Research. 2013; 100: 134–142.

[9] Wang M, Yang H, Zheng L, Zhang Z, Tang Y, Wang G, *et al*. Downregulation of TMEM16a calcium-activated chloride channel contributes to cerebrovascular remodeling during hypertension by promoting basilar smooth muscle cell proliferation. Circulation. 2012; 125: 697–707.

[10] Hwang T, Yeh J, Zhang J, Yu Y, Yeh H, Destefano S. Structural mechanisms of CFTR function and dysfunction. The Journal of General Physiology. 2018; 150: 539–570.

[11] Super M, Irtiza-Ali A, Roberts SA, Schwarz M, Young M, Smith A, *et al*. Blood pressure and the cystic fibrosis gene: evidence for lower pressure rises with age in female carriers. Hypertension. 2004; 44: 878–883.

[12] Zhang Y, Ye LL, Yuan H, Duan DD. CFTR plays an important role in the regulation of vascular resistance and high-fructose/salt-diet induced hypertension in mice. Journal of Cystic Fibrosis. 2021; 20: 516–524.

[13] Wallace HL, Southern KW, Connell MG, Wray S, Burdyga T. Abnormal tracheal smooth muscle function in the CF mouse. Physiological Reports. 2013;1: e00138.

[14] Vandebrouck C, Melin P, Norez C, Robert R, Guibert C, Mettey Y, *et al*. Evidence that CFTR is expressed in rat tracheal smooth muscle cells and contributes to bronchodilation. Respiratory Research. 2006; 7: 113.

[15] Peter BF, Lidington D, Harada A, Bolz HJ, Vogel L, Heximer S, *et al*. Role of sphingosine-1-phosphate phosphohydrolase 1 in the regulation of resistance artery tone. Circulation Research. 2008; 103: 315–324.

[16] Robert R, Norez C, Becq F. Disruption of CFTR chloride channel alters mechanical properties and cAMP-dependent Cl- transport of mouse aortic smooth muscle cells. The Journal of Physiology. 2005; 568: 483–495.

[17] Govindaraju V, Michoud M, Ferraro P, Arkinson J, Safka K, Valderrama-Carvajal H, *et al*. The effects of interleukin-8 on airway smooth muscle contraction in cystic fibrosis. Respiratory Research. 2008; 9: 76.

[18] Lidington D, Fares JC, Uhl FE, Dinh DD, Kroetsch JT, Sauvé M, *et al*. CFTR Therapeutics Normalize Cerebral Perfusion Deficits in Mouse Models of Heart Failure and Subarachnoid Hemorrhage. JACC: Basic to Translational Science. 2019; 4: 940–958.

[19] Lang P, Bai J, Zhang Y, Yang X, Xia Y, Lin Q, *et al*. Blockade of intercellular adhesion molecule-1 prevents angiotensin II-induced hypertension and vascular dysfunction. Laboratory Investigation. 2020; 100: 378–386.

[20] Lara LS, McCormack M, Semprum-Prieto LC, Shenouda S, Majid DSA, Kobori H, *et al*. At1 receptor-mediated augmentation of angiotensinogen, oxidative stress, and inflammation in ANG II-salt hypertension. American Journal of Physiology. Renal Physiology. 2012; 302: F85–F94.

[21] Ma M, Gao M, Guo K, Wang M, Li X, Zeng X, *et al*. TMEM16a Contributes to Endothelial Dysfunction by Facilitating Nox2 NADPH Oxidase-Derived Reactive Oxygen Species Generation in Hypertension. Hypertension. 2017; 69: 892–901.

[22] Liu C, Li F, Lv X, Ma M, Li X, Lin C, *et al*. Endophilin a2 regulates calcium-activated chloride channel activity via selective autophagy-mediated TMEM16a degradation. Acta Pharmacologica Sinica. 2020; 41: 208–217.

[23] Tabeling C, Yu H, Wang L, Ranke H, Goldenberg NM, Zabini D, *et al*. CFTR and sphingolipids mediate hypoxic pulmonary vasoconstriction. Proceedings of the National Academy of Sciences of the United States of America. 2015; 112: E1614–E1623.

[24] Smutny T, Dusek J, Hyrsova L, Nekvindova J, Horvatova A, Micuda S, *et al*. The 3′-untranslated region contributes to the pregnane X receptor (PXR) expression down-regulation by PXR ligands and up-regulation by glucocorticoids. Acta Pharmaceutica Sinica B. 2020; 10: 136–152.

[25] Zhao L, Li J, Huang X, Wang G, Lv X, Meng W, *et al*. Xyloketal B exerts antihypertensive effect in renovascular hypertensive rats via the no-sGC-cGMP pathway and calcium signaling. Acta Pharmacologica Sinica B. 2018; 39: 875–884.

[26] Wang G, Qian Y, Qiu Q, Lan X, He H, Guan Y. Interaction between Cl- channels and CRAC-related Ca2+ signaling during T lymphocyte activation and proliferation. Acta Pharmacologica Sinica B. 2006; 27: 437–446.

[27] Cai B, Li X, Chen J, Tang Y, Wang G, Zhou J, *et al*. Ginsenoside-Rd, a new voltage-independent Ca2+ entry blocker, reverses basilar hypertrophic remodeling in stroke-prone renovascular hypertensive rats. European Journal of Pharmacology. 2009; 606: 142–149.

[28] Khasnis M, Nakatomi A, Gumpper K, Eto M. Reconstituted human myosin light chain phosphatase reveals distinct roles of two inhibitory phosphorylation sites of the regulatory subunit, MYPT1. Biochemistry. 2014; 53: 2701–2709.

[29] Perez A, Issler AC, Cotton CU, Kelley TJ, Verkman AS, Davis PB. CFTR inhibition mimics the cystic fibrosis inflammatory profile. American Journal of Physiology. Lung Cellular and Molecular Physiology. 2007; 292: L383–95.

[30] Sellers ZM, Kovacs A, Weinheimer CJ, Best PM. Left ventricular and aortic dysfunction in cystic fibrosis mice. Journal of Cystic Fibrosis. 2013; 12: 517–24.

[31] Jiang K, Jiao S, Vitko M, Darrah R, Flask CA, Hodges CA, *et al*. The impact of Cystic Fibrosis Transmembrane Regulator Disruption on cardiac function and stress response. Journal of Cystic Fibrosis. 2016; 15: 34–2.

[32] Xiang SY, Ye LL, Duan LM, Liu L, Ge Z, Auchampach JA, *et al*. Characterization of a critical role for CFTR chloride channels in cardioprotection against ischemia/reperfusion injury. Acta Pharmacologica Sinica B. 2011; 32: 824–833.

[33] Liu Y, Lin Z, Liu M, Liao H, Chen Y, Zhang X, *et al*. CFTR deficiency causes cardiac dysplasia during zebrafish embryogenesis and is associated with dilated cardiomyopathy. Mechanisms of Development. 2020; 163: 103627.

[34] James AF. Enigmatic variations: the many facets of CFTR function in the heart. Acta Physiologica. 2020; 230: e13525.

[35] Peotta VA, Bhandary P, Ogu U, Volk KA, Roghair RD. Reduced blood pressure of CFTR-F508del carriers correlates with diminished arterial reactivity rather than circulating blood volume in mice. Public Library of Science One. 2014; 9: e96756.

[36] Wei X, Lu Z, Yang T, Gao P, Chen S, Liu D, *et al*. Stimulation of Intestinal Cl- Secretion through CFTR by Caffeine Intake in Salt-Sensitive Hypertensive Rats. Kidney & Blood Pressure Research. 2018; 43: 439–448.

[37] Vizzardi E, Sciatti E, Bonadei I, Menotti E, Prati F, Scodro M, *et al*. Elastic aortic properties in cystic fibrosis adults without cardiovascular risk factors: a case-control study. Echocardiography. 2019; 36: 1118–1122.

[38] Guo JJ, Stoltz DA, Zhu V, Volk KA, Segar JL, McCray PB, *et al*. Genotype-specific alterations in vascular smooth muscle cell function in cystic fibrosis piglets. Journal of Cystic Fibrosis. 2014; 13: 251–259.

[39] Rabbani G, Vijay V, Sarabu MR, Gupte SA. Regulation of human internal mammary and radial artery contraction by extra-

cellular and intracellular calcium channels and cyclic adenosine 3', 5' monophosphate. The Annals of Thoracic Surgery. 2007; 83: 510–515.

[40] Bozoky Z, Ahmadi S, Milman T, Kim TH, Du K, Di Paola M, *et al*. Synergy of cAMP and calcium signaling pathways in CFTR regulation. Proceedings of the National Academy of Sciences of the United States of America. 2017; 114: E2086–E2095.

[41] Walsh DE, Harvey BJ, Urbach V. CFTR regulation of intracellular calcium in normal and cystic fibrosis human airway epithelia. The Journal of Membrane Biology. 2000; 177: 209–219.

[42] Balghi H, Robert R, Rappaz B, Zhang X, Wohlhuter-Haddad A, Evagelidis A, *et al*. Enhanced Ca2+ entry due to Orai1 plasma membrane insertion increases IL-8 secretion by cystic fibrosis airways. The Federation of American Societies for Experimental Biology Journal. 2011; 25: 4274–4291.

[43] Martins JR, Kongsuphol P, Sammels E, Dahimène S, Aldehni F, Clarke LA, *et al*. F508del-CFTR increases intracellular Ca (2+) signaling that causes enhanced calcium-dependent Cl (-) conductance in cystic fibrosis. Biochimica Et Biophysica Acta. 2011; 1812: 1385–1392.

[44] Wynne BM, Chiao C, Webb RC. Vascular Smooth Muscle Cell Signaling Mechanisms for Contraction to Angiotensin II and Endothelin-1. Journal of the American Society of Hypertension. 2009; 3: 84–95.

[45] Huang W, Tan M, Wang Y, Liu L, Pan Y, Li J, *et al*. Increased intracellular Cl- concentration improves airway epithelial migration by activating the RhoA/ROCK Pathway. Theranostics. 2020; 10: 8528–8540.

[46] Chipperfield AR, Harper AA. Chloride in smooth muscle. Progress in Biophysics and Molecular Biology. 2000; 74: 175–221.

[47] Bulley S, Neeb ZP, Burris SK, Bannister JP, Thomas-Gatewood CM, Jangsangthong W, *et al*. TMEM16a/ANO1 channels contribute to the myogenic response in cerebral arteries. Circulation Research. 2012; 111: 1027–1036.

[48] Dam VS, Boedtkjer DMB, Nyvad J, Aalkjaer C, Matchkov V. TMEM16a knockdown abrogates two different Ca (2+)-activated Cl (-) currents and contractility of smooth muscle in rat mesenteric small arteries. Pflugers Archiv. 2014; 466: 1391–1409.

[49] Heinze C, Seniuk A, Sokolov MV, Huebner AK, Klementowicz AE, Szijártó IA, *et al*. Disruption of vascular Ca2+-activated chloride currents lowers blood pressure. The Journal of Clinical Investigation. 2014; 124: 675–686.

[50] Manoury B, Tamuleviciute A, Tammaro P. TMEM16a/Anoctamin 1 protein mediates calcium-activated chloride currents in pulmonary arterial smooth muscle cells. The Journal of Physiology. 2010; 588: 2305–2314.

Supplementary material: Supplementary material associated with this article can be found, in the online version, at https://www.imrpress.com/journal/FBL/26/12/10.52586/5034.

Abbreviations: Ang II, angiotensin II; VSMCs, vascular smooth muscle cells; CaCC, Ca^{2+}-activated Cl^- channel; VRCC, volume regulated Cl^- channel; CFTR, cystic fibrosis transmembrane conductance regulator; CF, cystic fibrosis; SBP, systolic blood pressure; DBP, diastolic blood pressure; MLC, myosin light chain; MLCK, myosin light chain kinase; MLCP, myosin light chain phosphatase; PLC, phospholipase C; IP_3, inositol trisphosphate; DAG, diacylglycerol; SR, sarcoplasmic reticulum; PKC, protein kinase C; $[Ca^{2+}]_i$, intracellular Ca^{2+} concentration; CaM, calmodulin; SHR, spontaneously hypertensive rat; 2k2c, 2-kidney 2-clip; t-MLC, total myosin light chain; p-MLC, phosphorylated myosin light chain; MYPT1, myosin phosphatase target subunit 1; p-MYPT1, phosphorylated MYPT1; L-NAME, L-nitro-arginine methyl ester; HBSS, Hanks' Balanced Salt Solution; PVDF, polyvinylidene difluoride; DMEM/F12, Dulbecco's modified Essential medium/F-12; BASMCs, basilar artery smooth muscle cells; PKA, protein kinase A; SOCC, store-operated calcium channel.

Keywords: CFTR; Hypertension; Vasoconstriction; Vascular smooth muscle cells; Ca^{2+}; RhoA

Send correspondence to:

Guanlei Wang, Department of Pharmacology, Zhongshan School of Medicine, Sun Yat-sen University, 510080 Guangzhou, Guangdong, China, E-mail: wangglei@mail.sysu.edu.cn

Bin Zhang, Guangdong Cardiovascular Institute, Guangdong Provincial People's Hospital, Guangdong Academy of Medical Sciences, 510080 Guangzhou, Guangdong, China, E-mail: drbinzhang@gdph.org.cn

† These authors contributed equally.